THE JOURNAL OF BIOLOGICAL CHEMISTRY
Vol. 270, No. 15, Issue of April 14, pp. 8528–8535, 1995
Printed in U.S.A.

Region-specific Activity of the Plasma Membrane Ca^{2+} Pump and Delayed Activation of Ca^{2+} Entry Characterize the Polarized, Agonist-evoked Ca^{2+} Signals in Exocrine Cells*

(Received for publication, January 3, 1995, and in revised form, January 31, 1995)

Emil C. Toescu‡ and Ole H. Petersen

From the Physiological Laboratory, Liverpool University, L69 3BX, Liverpool, United Kingdom

The initial release of Ca^{2+} from the intracellular Ca^{2+} stores is followed by a second phase during which the agonist-dependent Ca^{2+} response becomes sensitive to the extracellular Ca^{2+}, indicating the involvement of the plasma membrane (PM) Ca^{2+} transport systems. The time course of activation of these transport systems, which consist of both Ca^{2+} extrusion and Ca^{2+} entry pathways, is not well established. To investigate the participation of these processes during the agonist-evoked Ca^{2+} response, isolated pancreatic acinar cells were exposed to maximal concentrations of an inositol 1,4,5-trisphosphate-mobilizing agonist (acetylcholine, 10 μM) in different experimental conditions. Following the increase of $[Ca^{2+}]_i$, there was an almost immediate activation of the PM Ca^{2+} extrusion system, and maximal activity was reached within less than 2 s. The rate of Ca^{2+} extrusion was dependent on the level of $[Ca^{2+}]_i$, with a steep activation at values just above the resting $[Ca^{2+}]_i$ and reached a plateau value at 700 nM Ca^{2+}. In contrast, the PM Ca^{2+} entry pathway was activated with a much slower time course. There was also a delay of 3–4 s between the maximal effective depletion of the intracellular Ca^{2+} stores and the activation of this entry pathway. By use of digital imaging data, the PM Ca^{2+} transport systems were also analyzed independently in two regions of the cells, the lumenal and the basal poles. With respect to the activation of the Ca^{2+} entry pathways, no significant difference existed between these two regions. In contrast, the PM Ca^{2+} pump displayed a different pattern of activity in these regions. In the basal pole, the pump activity was more sensitive to changes of $[Ca^{2+}]_i$ and had a higher maximal activity. Also, in the lumenal pole, the pump became saturated at values of $[Ca^{2+}]_i$ around 700 nM, whereas at the basal pole $[Ca^{2+}]_i$ had a biphasic effect on the pump activity, and higher $[Ca^{2+}]_i$ inhibited the pump. It is argued that these differences in sensitivity to the levels of $[Ca^{2+}]_i$ and the different relationship between $[Ca^{2+}]_i$ and the rate of extrusion at the two functional poles of the pancreatic acinar cells indicate that the plasma membrane Ca^{2+}ATPase might play an important role in the polarization of the Ca^{2+} response.

In many cell types stimulation by agonists which enhance the production of $InsP_3$[1] initiate a complex succession of events which culminate with the release of Ca^{2+} from intracellular stores (1). In exocrine cells, digital Ca^{2+} imaging techniques revealed that this release shows a spatial polarization which mirrors the functional polarization characteristic for these cells (2–6). This spatial organization of the Ca^{2+} signal, which involves an initial increase in the lumenal pole followed by a spreading of a Ca^{2+} tide toward the basolateral regions, can be evoked either by agonist stimulation (2, 4, 7) or by direct intracellular perfusion of $InsP_3$ (6, 8). We have shown recently that this polarization is not due to a difference in the kinetic properties of the Ca^{2+} release process in the two regions of the cell (7). An important functional mechanism underlying this polarization is the heterogeneity in the sensitivity of the intracellular Ca^{2+} pools to the actions of the Ca^{2+} releasing agents (6–10). However, we reported previously that the intracellular Ca^{2+} buffers have also an important role in the regulation of the agonist-evoked Ca^{2+} signals (11, 12). In a more general definition, these Ca^{2+} buffers include not only the cytosolic Ca^{2+}-binding proteins, already implicated in a model of "dynamic decoding" (13), but also the systems involved in the removal of Ca^{2+} from the cytosol. Among the latter, the PM Ca^{2+}ATPase is an established contender, shown to extrude a substantial amount of Ca^{2+} following the agonist-evoked Ca^{2+} signals (14).

The initial release of Ca^{2+} is followed by a second phase of the Ca^{2+} response, sensitive to the manipulation of extracellular Ca^{2+}. In the absence of extracellular Ca^{2+} maximal agonist stimulation still evokes an increase of $[Ca^{2+}]_i$, but only transient, due to the activation of the Ca^{2+} extrusion mechanisms, represented in pancreatic acinar cells mainly by the PM Ca^{2+}ATPase (14, 15). In the presence of extracellular Ca^{2+}, the extrusion of Ca^{2+} is balanced by an entry of Ca^{2+} from the external medium, the two processes resulting in a maintained, steady-state plateau of increased $[Ca^{2+}]_i$. Several lines of evidence, brought together into the model of capacitative Ca^{2+} entry (16, 17), point to the fact that the activation of the Ca^{2+} entry pathway is a consequence of the depletion of the intracellular Ca^{2+} pools. Regarding the nature of this Ca^{2+} pathway, several patch clamp studies (18, 19) identified a Ca^{2+}-release-activated Ca^{2+} current (I_{CRAC}). What is still very much a matter of debate is the question of how the depletion of the stores is transduced into the activation of the Ca^{2+} entry channel and numerous hypotheses have been proposed to account for this process. These include models of "mechanical coupling" involving direct interactions between the $InsP_3$-sensitive Ca^{2+} release channel/receptor and the Ca^{2+} entry pathway mediated through an $InsP_4$ receptor (20) or through the cytoskeleton (17). Other "metabolic coupling" models propose that the activation of the Ca^{2+} entry pathway is the result of either (*a*) the stimulation of certain metabolic pathways, such as the cytochrome

* The work was funded by grants from the Medical Research Council. The costs of publication of this article were defrayed in part by the payment of page charges. This article must therefore be hereby marked "*advertisement*" in accordance with 18 U.S.C. Section 1734 solely to indicate this fact.

‡ To whom correspondence should be addressed: Dept. of Physiology, The School of Medicine, Edgbaston, Birmingham B15 2TT, UK.

[1] The abbreviations used are: $InsP_3$, inositol 1,4,5-trisphosphate; $InsP_4$, inositol 1,3,4,5-tetrakiphosphate; PM, plasma membrane.

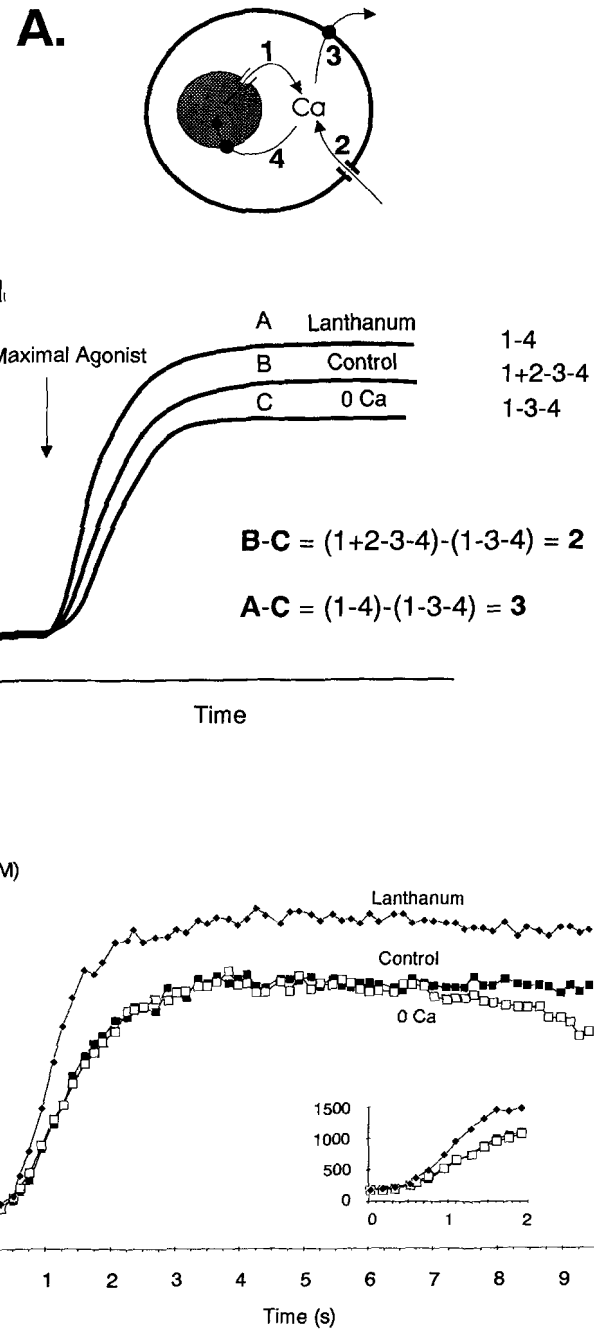

FIG. 1. **Principles of analysis.** *A*, schematic representation of the Ca^{2+} transport systems involved during the agonist-evoked Ca^{2+} signaling. *Process 1* represents the release of Ca^{2+} from the intracellular pools; *process 2*, the Ca^{2+} entry pathway; *process 3*, the plasma membrane Ca^{2+} extrusion system; and *process 4*, the reuptake of Ca^{2+} into the internal stores. *B*, schematic representation of the experimental traces. Information about the Ca^{2+} entry and/or Ca^{2+} extrusion pathways can be derived by simple algebraic summation of individual processes (see text for further details). *C*, actual experimental traces of $[Ca^{2+}]_i$ following maximal stimulation with acetylcholine (10 μM). The values plotted represent mean values for each time point derived from: *Lanthanum*, four separate experiments (31 cells); *Control*, six separate experiments (65 cells); *0 Ca*, five experiments (54 cells). Time $t = 0$ represents the time of the first increase in $[Ca^{2+}]_i$ for each individual cell and defined under "Materials and Methods." For clarity, the error bars were omitted (for each time point they represent 10–20% of the mean value). The *inset* shows, on an expanded time scale, the first 2 s of the Ca^{2+} response.

P450 (21) or the NO/cGMP (22), (*b*) the release of a diffusible messenger (the "Ca^{2+} influx factor" (23)), or (*c*) the activation of small GTP-binding proteins (19, 24) or tyrosine kinase(s) (25). The analysis is further complicated by the fact that in some cell types, such as the hepatocytes, agonist stimulation activates several Ca^{2+} entry pathways (26, 27). An important parameter which could help in differentiating between these various proposals is that of the temporal relationship between the depletion of the Ca^{2+} pools and the activation of the Ca^{2+} entry pathway.

In the present study digital Ca^{2+} imaging technologies were used to investigate the spatial and temporal aspects of the activation of the plasma membrane Ca^{2+} transport systems following the maximal stimulation of the pancreatic acinar cells by an $InsP_3$-mobilizing agonist. The main conclusions of this study are that (*a*) the temporal activation of the Ca^{2+} extrusion system is very different from that of the Ca^{2+} entry pathway, (*b*) the activation of the Ca^{2+} entry pathway is significantly delayed in respect to the mobilization of Ca^{2+} from the intracellular pools, and (*c*) the PM Ca^{2+} pump display different patterns of activity in different regions of the cell, which could be an important mechanism in the polarization of the Ca^{2+} signal.

MATERIALS AND METHODS

Preparation of Cells—Individual cells and small clusters of acinar cells were obtained from isolated mouse pancreata by enzymatic dispersion in a water bath at 37 °C as described previously (4). Briefly, the intact glands were injected with a collagenase solution (200 units/ml, Worthington), incubated for 7–15 min, and finally manually agitated to yield the isolated cell preparation. Throughout the preparation procedure and subsequently in some experiments, a buffer solution ("control" solution) containing (mM): NaCl 140, KCl 4.7, $CaCl_2$ 1.1, $MgCl_2$ 1.1, glucose 10, and HEPES 10 (pH 7.2 adjusted with NaOH) with an osmolality of 295 mOsm/liter was used. For some experiments a "0 Ca" solution was used which consisted of a nominally Ca^{2+}-free control solution to which 0.5 mM EGTA was added. To inhibit all the plasma membrane Ca^{2+} transport systems (28), 1 mM La^{3+} was added to the

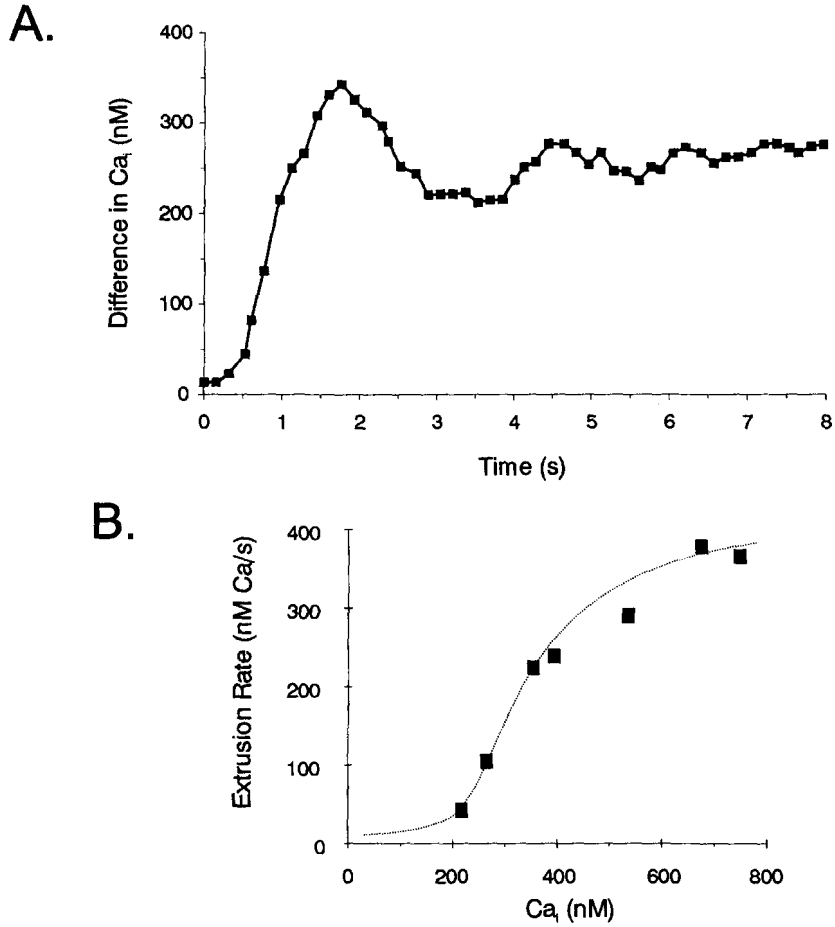

FIG. 2. **Participation of the Ca^{2+} extrusion system during the agonist-evoked Ca^{2+} signal.** *A*, plot of the time course of activation of the PM Ca^{2+} extrusion system. Data are presented as the difference in $[Ca^{2+}]_i$ due to the activation of this system and was derived by subtracting, for each individual time point, the $[Ca^{2+}]_i$ values recorded in the presence of La^{3+} from those obtained in the absence of extracellular Ca^{2+} (see Fig. 1). *B*, relationship between the apparent rate of Ca^{2+} extrusion and the value of $[Ca^{2+}]_i$ at which that rate was recorded. The apparent extrusion rate (ordinate) was calculated as the difference in mean $[Ca^{2+}]_i$ values between two consecutive time points ($d[Ca^{2+}]_i$) shown in *Panel A* and divided by the respective time interval (dt). These values for the extrusion rate are plotted against the actual $[Ca^{2+}]_i$ levels (on the *abscissa*) at which the rate was calculated. The values plotted on the abscissa are the values of $[Ca^{2+}]_i$ recorded in the absence of extracellular Ca^{2+}, condition in which the PM Ca^{2+}ATPase is active.

control solution ("lanthanum" solution).

Ca^{2+} Imaging and Data Analysis—Cells were loaded with 1 μM fura-2-AM for 30 min at room temperature, washed twice, and used within 3–4 h. During experiments, the cells, placed on a glass coverslip attached to an open perfusion chamber, were continuously perifused from a gravity-fed perifusion system.

The images were captured using a Nikon Diaphot inverted microscope, an intensified charge coupled device camera (Photonic Science Inc.) and recorded on a MagiCal station (Applied Imaging, UK). Other details of the Ca^{2+} imaging were described previously (9). The fluorescence signals were captured, at video-frame rate (0.16-s intervals between two true ratio images) with a 20× magnification objective. In each field, comprising several cells, those cells responding to agonist were analyzed by calculating the mean $[Ca^{2+}]_i$ value within areas defined with a light-sensitive pen on a bright field image showing the morphology of cells. The areas used for these measurements were of a similar size to those used by us previously (4, 9). Due to biological variability and to the inherently variable geometry of our perifusion method, the lag time between the start of agonist application and the initiation of Ca^{2+} response varied from one experiment to another. To compare agonist-evoked Ca^{2+} signals in different experiments we have chosen to normalize the Ca^{2+} signal to the first time point of the $[Ca^{2+}]_i$ increase (defined as the first point of increase of $[Ca^{2+}]_i$ which is followed by two consecutive higher values of $[Ca^{2+}]_i$).

Fura-2 fluorescence was calibrated using the cells loaded in the normal way and perfused subsequently either with 10 mM EGTA or with 10 mM Ca^{2+}, in the presence of 2 mM ionomycin. The dissociation constant for fura 2 (K_d) used for the calculation of the Ca^{2+} values was 224 nM.

Other Materials—Chemicals were purchased from Merck-BDH (UK) and Sigma (UK) except fura-2 which was obtained from Novo-Calbiochem (UK).

RESULTS

General Method of Analysis—Fig. 1*A* depicts schematically the major Ca^{2+} transport processes which participate in establishing the value of $[Ca^{2+}]_i$ during the agonist-evoked, $InsP_3$-mediated Ca^{2+} signaling in nonexcitable cells. Clearly, in such studies which measure the resultant $[Ca^{2+}]_i$, the direct and separate assessment of the participation of each process to the overall $[Ca^{2+}]_i$ value is not possible. Nevertheless, by using certain experimental conditions and by performing simple algebraic additions as shown in Fig. 1*B*, the relative participation of the plasma membrane Ca^{2+} transport systems can be ascertained. In the presence of maximal agonist stimulation and for the short duration (10 s) of these experiments, the $InsP_3$-activated Ca^{2+} release channel (Fig. 1*A*, *process 1*) is assumed to be continuously activated. In the absence of extracellular Ca^{2+} (Fig. 1*B*, *trace C*), the participation of the capacitative Ca^{2+} entry pathway (Fig. 1*A*, *process 2*) is eliminated. We have shown recently (28) that 1 mM La^{3+} effectively seals the cell with respect to extracellular Ca^{2+}, blocking both the entry and the extrusion of Ca^{2+} (Fig. 1*A*, *processes 2* and *3*, respectively) and results in an increased Ca^{2+} signal (28) (Fig. 1*C*). As shown in Fig. 1*B*, the difference between traces obtained in the presence of La^{3+} (*trace A*) and those obtained in the absence of extracellular Ca^{2+} (*trace C*) are due only to the activity of the plasma membrane Ca^{2+} ATPase. Similarly, subtraction of traces obtained in the absence of extracellular Ca^{2+} from traces obtained in control conditions (*trace B*) will provide information about the behavior of the Ca^{2+} entry pathway. Fig. 1*C* shows the actual experimental (mean) values, measured across the whole cell and normalized for the first value of increased $[Ca^{2+}]_i$ as detailed under "Materials and Methods."

Analysis of Plasma Membrane Ca^{2+} Transport Systems—The participation of the plasma membrane Ca^{2+} transport system was assessed for each time point, as the difference between the $[Ca^{2+}]_i$ measured in the presence of extracellular La^{3+} (1 mM) and in the absence of extracellular Ca^{2+} (Fig. 1*B*).

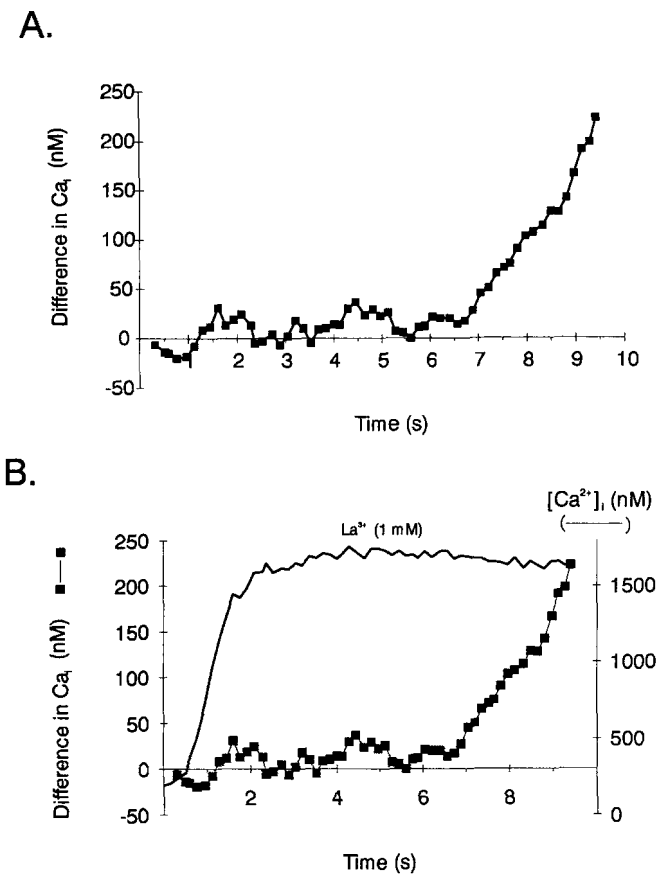

FIG. 3. **Delayed activation of the PM Ca^{2+} entry pathway.** *A*, plot of the time course of activation of the PM Ca^{2+} entry pathway. Data are presented as the difference between the values recorded in control conditions and in the absence of extracellular Ca^{2+}, when the Ca^{2+} entry pathway is inactive. *B*, the time course of the activation of the PM Ca^{2+} entry pathway (*filled squares, left ordinate*) is plotted together with the values of $[Ca^{2+}]_i$ recorded in the presence of La^{3+} (1 mM) (*line trace, right ordinate*).

In agreement with our previous suggestion (28), it appears that this Ca^{2+} transport system is activated very early during maximal agonist stimulation. Within 0.5 s the difference in $[Ca^{2+}]_i$ due to the PM Ca^{2+}ATPase is manifest, and it reaches a maximal level in less than 2 s (Fig. 2*A*), by which time it accounts for a difference of 350 nM Ca^{2+}. Throughout the rest of the stimulation the Ca^{2+} pump remains active. An important property of this transport system is illustrated in Fig. 2*B* which shows the relationship between the apparent extrusion rate, calculated from data shown in Fig. 2*A* as the difference (d) in $[Ca^{2+}]_i$ values per unit of time ($d[Ca^{2+}]_i/dt$), and the values of $[Ca^{2+}]_i$. The noteworthy feature of this relationship is its steepness: at values of $[Ca^{2+}]_i$ over 200 nM, even small changes in the value of $[Ca^{2+}]_i$ evoke big increases in the apparent rate of extrusion. At $[Ca^{2+}]_i$ values around 600 nM, the apparent rate is maximal (370 nM Ca^{2+}/s). Further increases of $[Ca^{2+}]_i$ do not determine any significant additional activation.

The activation of the Ca^{2+} entry pathway can be derived from the comparison between control experiments and those performed in the absence of extracellular Ca^{2+} (see Fig. 1*B*). It is apparent from Fig. 1*C* that the values of $[Ca^{2+}]_i$ measured in the first seconds after the beginning of $[Ca^{2+}]_i$ increase are, in pancreatic acinar cells, little affected by the absence of extracellular Ca^{2+}, and the two curves are almost superimposable. As shown in Fig. 3*A* the participation of the Ca^{2+} entry is significantly delayed, requiring more than 6 s for its activation. This time scale is to be contrasted with the time course of Ca^{2+} release from the intracellular Ca^{2+} pools following agonist stimulation (Fig. 3*B*). Since La^{3+} inhibits all Ca^{2+} transport across the plasma membrane (28, 36), the measured values of $[Ca^{2+}]_i$ in its presence reflect only the release from the intracellular Ca^{2+} pools. The trace plotted in Fig. 3*B* shows that, by 3 s, the $[Ca^{2+}]_i$ reached a steady-state level, maintained afterward. This steady-state level is the result of the maximal efflux of Ca^{2+} from the intracellular stores through the Ca^{2+} release channels balanced by the reuptake into the stores through the endoplasmic reticulum Ca^{2+}ATPase. As such, it represents a level of maximal "effective" depletion of the pools, which is thus completed by 3 s after the initiation of the Ca^{2+} release and precedes by 3–4 s the activation of the Ca^{2+} entry pathway.

Regional Analysis of Ca^{2+} Transport Activity during Polarized Ca^{2+} Signals—The use of Ca^{2+} imaging allows the analysis of changes in $[Ca^{2+}]_i$ in different regions of the cell. In many exocrine cells, the Ca^{2+} signal is initially localized to the lumenal pole from where, 0.3–0.5 s later, it spreads toward the basolateral pole. Using a similar methodology, we investigated the pattern of activation and the apparent kinetic properties of the PM Ca^{2+} transport in different regions of the pancreatic acinar cells.

Fig. 4*A* shows the mean increases in $[Ca^{2+}]_i$ recorded during the agonist-evoked Ca^{2+} signal in the lumenal pole of pancreatic acinar cells in the presence of La^{3+} or absence of extracellular Ca^{2+}, respectively. As in previous figures the data were normalized to the first increase in $[Ca^{2+}]_i$. From these results, the time course of the activation of the PM Ca^{2+} extrusion system at the lumenal pole was calculated and shown in Fig. 4*B*. In this figure the extrusion activity is plotted together with the "reference" $[Ca^{2+}]_i$ trace (*i.e.* that recorded in the absence of extracellular Ca^2, when the PM Ca^{2+}ATPase is active). The increase of $[Ca^{2+}]_i$ rapidly activates the extrusion system, and its activity is maximal in less than 2 s, by which time it accounts for a difference of about 200 nM Ca^{2+}. It can also be seen from Fig. 4*B* that the lumenal PM Ca^{2+}ATPase maintains the same level of activity despite further increases of $[Ca^{2+}]_i$. Using the same procedure, the activity of the PM Ca^{2+}ATPase in the basal pole of the cells was assessed. These values are plotted in Fig. 4*C* together with the corresponding reference $[Ca^{2+}]_i$ trace in that region of the cell. To allow a direct comparison of the activation curves between the two regions, the initial time point in this graph is represented by the first increase of $[Ca^{2+}]_i$ *not* in this region, but in the lumenal pole. In the present set of data, as in previously published reports (2, 4, 6, 8), the increase of $[Ca^{2+}]_i$ in the lumenal pole precedes that in the basal pole by 0.3–0.4 s. In striking contrast to the activity of the Ca^{2+} extrusion system in the lumenal pole (Fig. 4*B*), in the basal pole of the pancreatic acinar cells the activity of the pump, after being maximally stimulated within 1.5 s, is inhibited despite further increases of $[Ca^{2+}]_i$.

A direct comparison of the time course of the activation of the Ca^{2+} extrusion systems in the two regions of the cell is presented in Fig. 5*A* which illustrates better the important differences between these two activities. The apparent rate of Ca^{2+} extrusion activation in the basal pole of the cell is almost twice as great as that seen in the lumenal pole. This increased rate of activity is associated also with a greater maximal activity. Finally, whereas the apparent activity of the PM Ca^{2+} extrusion system in the lumenal pole remains largely constant, in the basal pole it decreases immediately following its peak of activation. As seen in Fig. 4*B*, this decrease of Ca^{2+} extrusion activity is associated with further increases in $[Ca^{2+}]_i$. The relationship between Ca^{2+} extrusion and $[Ca^{2+}]_i$ for the two regions of the cell is presented in Fig. 5*B*. Both the lumenal and the basal extrusion systems are activated by an increase of

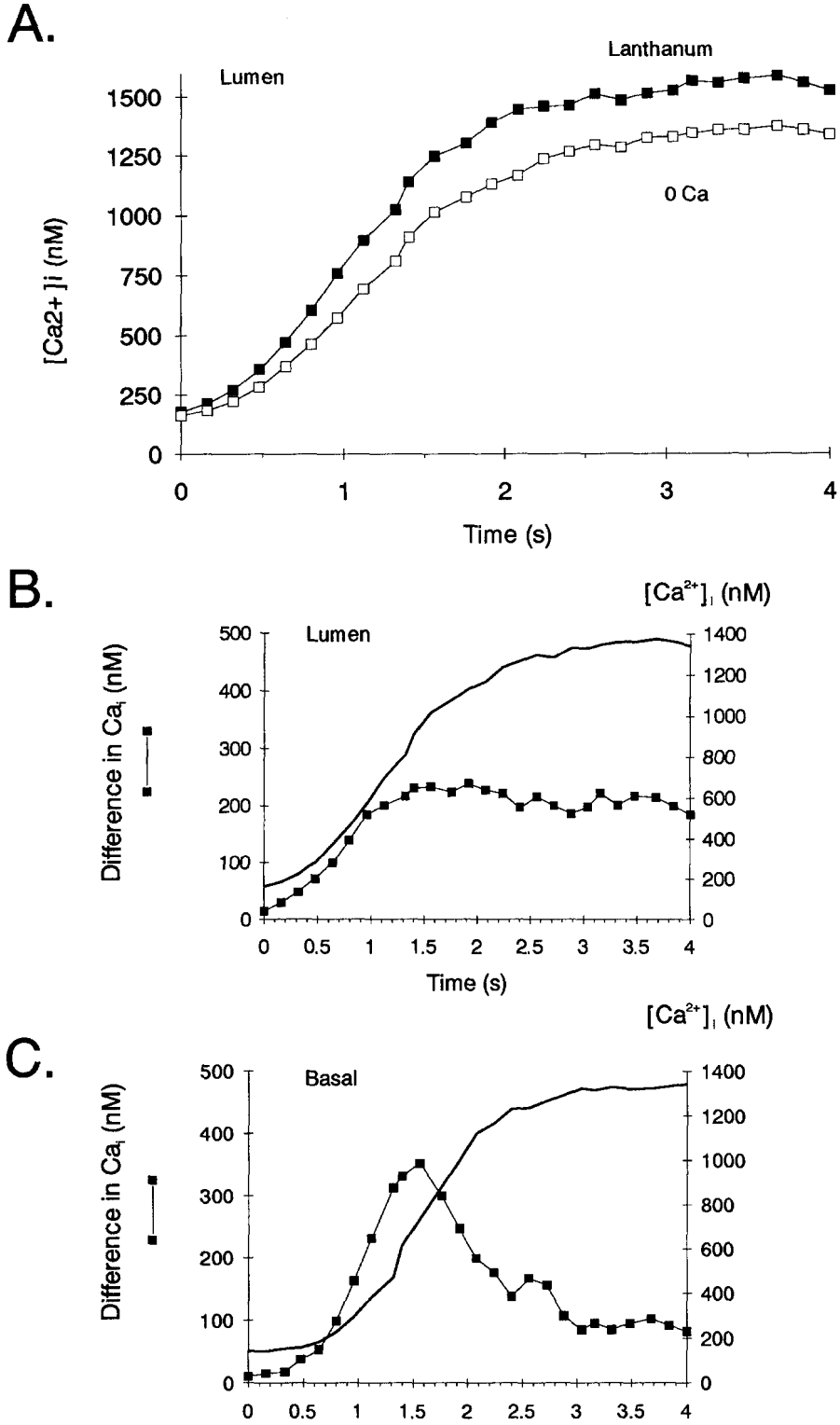

FIG. 4. **Regional analysis of the activity of the PM Ca^{2+} extrusion.** *A*, plot of the $[Ca^{2+}]_i$ values recorded in the lumenal pole. The two traces show mean $[Ca^{2+}]_i$ values from cells incubated in the presence of 1 mM La^{3+} (*closed squares*) or absence of extracellular Ca^{2+} (*open squares*). For this analysis some experiments were paired (performed successively, in the same day, with cells derived from the same animal). The data shown were derived from: *Lanthanum*, 7 experiments (27 cells); *0 Ca*, eight experiments (33 cells). *B*, plot of the time course of Ca^{2+} extrusion at the lumenal pole (*filled squares, left ordinate*), presented as the difference in $[Ca^{2+}]_i$ between the two traces shown in *Panel A* and the time course of $[Ca^{2+}]_i$ response (*line trace, right ordinate*) recorded at the same pole in the absence of extracellular Ca^{2+}. *C*, same data presentation as in *Panel B* but with the corresponding values for the basal pole of the cells.

$[Ca^{2+}]_i$, but the activation in the basal pole is much more sensitive to changes in $[Ca^{2+}]_i$. Thus, for increases of 100 nM Ca^{2+} above the resting $[Ca^{2+}]_i$ value, the extrusion in the lumenal pole will account for a Ca^{2+} difference of only 40 nM Ca^{2+}, whereas in the basal pole the difference is 150 nM Ca^{2+}. In both regions the extrusion systems reach a maximum activity at $[Ca^{2+}]_i$ around 0.7 μM, but the maximum value at the basal pole is higher than that in the lumenal pole. As discussed before, at higher values of $[Ca^{2+}]_i$ the extrusion in the two regions behave differently in respect to $[Ca^{2+}]_i$: whereas in the lumenal region the activity remains constant, in the basal pole further increases of $[Ca^{2+}]_i$ are associated with a decrease of extrusion, indicating an inhibitory effect of $[Ca^{2+}]_i$.

Next, the activation of the Ca^{2+} entry pathway was analyzed in a similar manner. Fig. 6*A* shows the mean $[Ca^{2+}]_i$ traces recorded in the lumenal pole in control conditions and in the absence of extracellular Ca^{2+}. From these traces the time course of Ca^{2+} entry activation was calculated and is shown in Fig. 6*B* (*filled squares*). Fig. 6*B* also shows that, in contrast to the activity of the PM Ca^{2+} extrusion system, there are no

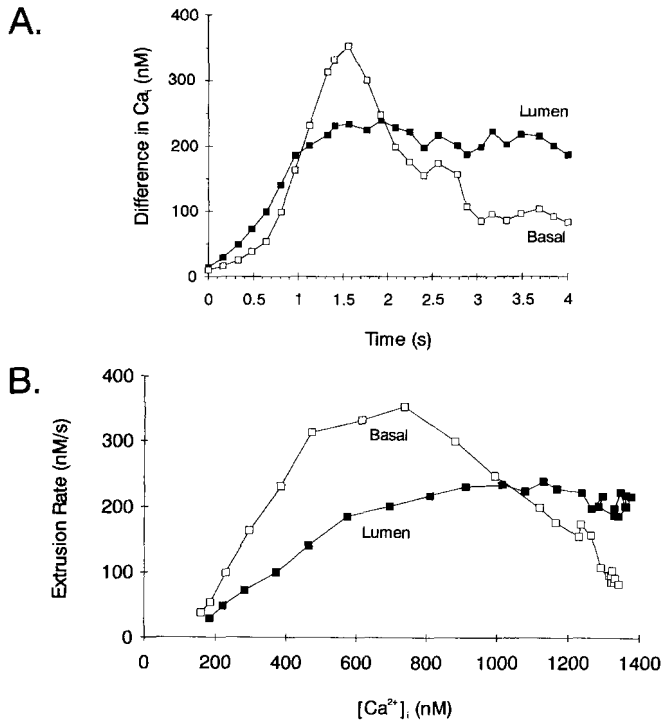

FIG. 5. **Differences in the activity of the PM CaATPase at the two poles of the pancreatic acinar cells.** *A*, direct comparison of the extrusion activity at the two poles: lumenal (*closed squares*) and basal (*open squares*). *B*, plot of the PM CaATPase apparent extrusion rate (calculated as described in legend to Fig. 2, *Panel B*) at the two poles of the cell against the values of $[Ca^{2+}]_i$. The values plotted on the *abscissa* are the values of $[Ca^{2+}]_i$ recorded in the absence of extracellular Ca^{2+}, a condition in which the PM CaATPase is active.

significant differences in the activation of the PM Ca^{2+} entry pathway between the lumenal and basal poles of the pancreatic acinar cells.

DISCUSSION

Two main conclusions emerge from the present results. The first one is that, following maximal agonist stimulation, the time course of activation of the two major PM Ca^{2+} transport systems, *i.e.* the extrusion and the entry pathway, is significantly different, with the Ca^{2+} entry pathway becoming active more than 5 s after the initiation of the Ca^{2+} release from the intracellular Ca^{2+} pools. Second, it is shown that the polarization of the Ca^{2+} signal, reported previously for several cell types (2–5, 29), is associated with significant differences in the activity of the PM Ca^{2+} extrusion system in two functionally distinct regions of the pancreatic acinar cells, the lumenal and the basal pole.

The question of the participation of the plasma membrane Ca^{2+} transport systems during the agonist-evoked Ca^{2+} signal is still debated. The entry of Ca^{2+} into cells along a strong electrochemical gradient is regulated by a variety of mechanisms (30). In electrically nonexcitable cells a salient feature of this process is that the depletion of the intracellular Ca^{2+} pools activates a Ca^{2+} entry pathway (16). The molecular nature of this Ca^{2+} entry pathway and, more importantly, the mechanisms which activate it are the subject of intensive research.

In some cell types, the burst of $[Ca^{2+}]_i$ increase during threshold or maximal stimulation is preceded by a slow pacemaker elevation of $[Ca^{2+}]_i$ (31–33). Recently, it has been proposed that an important component of this phase is the entry of external Ca^{2+} (34). This view extends a previous model (1, 35) in which it is proposed that an influx of external Ca^{2+} is an essential primer for the ensuing $[Ca^{2+}]_i$ increase. This primer Ca^{2+} initially loads the intracellular pools and subsequently sensitize the Ca^{2+} release process eventually determining the sudden release of Ca^{2+} from the endoplasmic reticulum. Implicit in this model is the fact that the pools are initially depleted of Ca^{2+}. The situation in the pancreatic acinar cells appears somewhat different. Stimulation of cells in the presence of lanthanum at a concentration which effectively seals these cells from the extracellular Ca^{2+} (28, 36) evokes an increase of $[Ca^{2+}]_i$ which is more rapid and of higher amplitude than in the absence of extracellular Ca^{2+} (Fig. 1) (28) indicating that the $InsP_3$-sensitive stores are fully Ca^{2+}-loaded. In addition, treatment with thapsigargin evokes, even in the absence of extracellular Ca^{2+}, increases of $[Ca^{2+}]_i$. Finally, as shown in Fig. 3, the activation of Ca^{2+} entry appears a few seconds after the maximal release of Ca^{2+} from the stores. This delayed activation has also been suggested previously, in experiments using short $0Ca^{2+}$ pulses during the increase of $[Ca^{2+}]_i$ following thapsigargin exposure (28). The delay in Fig. 3 indicates another important feature: the entry is not activated directly as a consequence of pool depletion. The length of this delay (3–5 s) exclude, at least for this cell type, a number activation mechanisms, including a direct receptor-regulated Ca^{2+} channel (37) or the participation of a plasma membrane, $InsP_3$-activated Ca^{2+} channel (38–40), and suggests the existence of a metabolic step interposed between store depletion and Ca^{2+} entry activation. The nature of this process is yet unclear. One proposal involves the cytochrome P450 (21), but more recent evidence seem to argue strongly against it (*e.g.* see Ref. 41). Other possibilities include the (paracrine) mediation by a Ca^{2+}-influx factor (23) or the participation of small G-proteins (19, 24).

In pancreatic acinar cells, the main Ca^{2+} extrusion system is represented by the PM Ca^{2+}ATPase since the participation of the Na^+/Ca^{2+} exchanger is minimal (14, 15). The present data show that this system, which is extremely powerful (14), is rapidly activated following agonist stimulation, in a manner dependent on $[Ca^{2+}]_i$ (Fig. 2*B*). An important feature of this dependence is its steepness: even small increases of $[Ca^{2+}]_i$ above the resting values induce significant increases in the pump activity.

Analysis of the PM Ca^{2+} extrusion in different regions of the cell revealed that the apparent activity of the pump is different. Pancreatic acinar cells, like many other cell types, display a polarization of the Ca^{2+} signal (2, 4). This polarization could be explained on the basis of differential sensitivity of intracellular Ca^{2+} stores to the action of the Ca^{2+} releasing agents (6, 8, 10). This hypothesis is supported by recent immunolocalization data showing a preferential localization of the $InsP_3$ receptor type 3 to the lumenal pole (42). An alternative mechanism, not exclusive of the first, is the existence of a differential buffering in different regions of the cell. Intracellular addition of mobile, high capacity, low affinity Ca^{2+} buffers induce significant changes in the pattern of Ca^{2+} oscillations (11). *In situ* cytosolic Ca^{2+} buffers have been invoked in a model explaining the characteristics of the interspike period (43). We have also proposed that the status of intracellular Ca^{2+} buffers play an important role in determining the specific pattern of Ca^{2+} oscillations independent of the nature of the agonist (12). In this context, the PM Ca^{2+} extrusion system can be seen as an effective cytosolic Ca^{2+} buffer. The different activities in the two poles of the pancreatic acinar cells might play an important role in the generation of the polarity of Ca^{2+} signal. Thus, even with a homogenous release of Ca^{2+} across the cytosol, the more rapid activation of the pump and its higher level of activity in the basal pole would explain the delay in the rise of $[Ca^{2+}]_i$ at this pole. Recent molecular biology studies showed that the

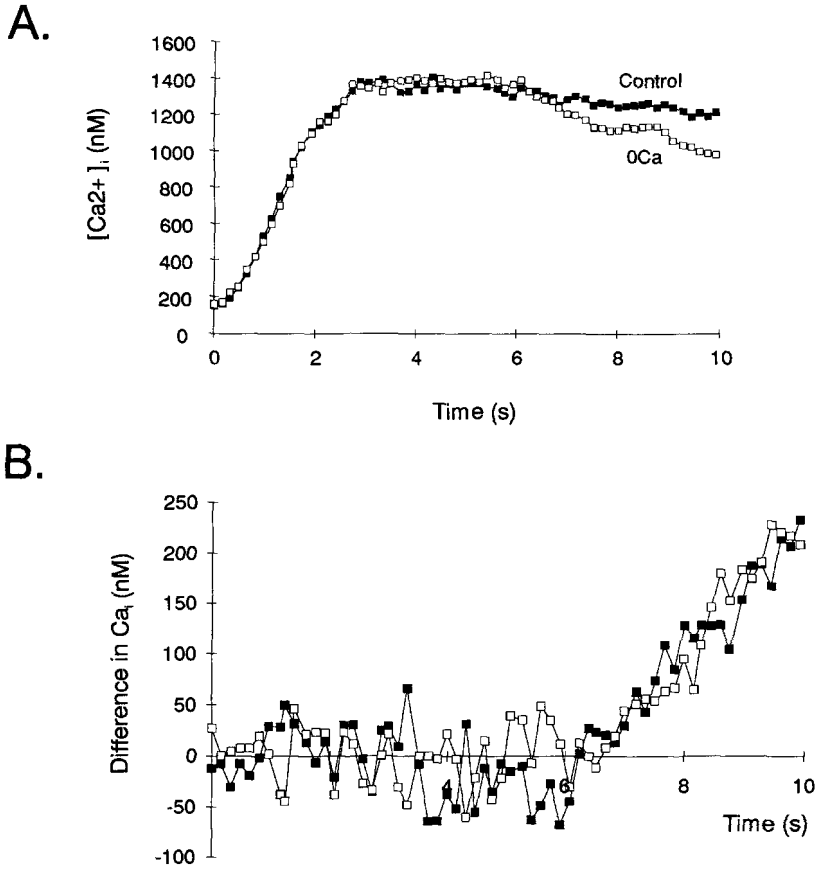

FIG. 6. **Regional analysis of the activity of the PM Ca^{2+} entry pathway.** *A*, plot of the $[Ca^{2+}]_i$ values recorded in the lumenal pole. The two traces show mean $[Ca^{2+}]_i$ values from cell incubated in Control conditions (*closed squares*) or absence of intracellular Ca^{2+} (*open squares*). For this analysis, some experiments were paired (in the sense described in the legend to Fig. 4), and the data shown were derived from: *Control*, seven experiments (52 cells); *0 Ca*, six experiments (29 cells). *B*, plot of Ca^{2+} entry (presented as the difference in $[Ca^{2+}]_i$) at both poles of the cell: lumenal (*filled squares*) and basal (*open squares*).

generic PM Ca^{2+}ATPase is in fact a large multigene family (PMCA family) (44). To date, little is known about the differences in functional properties between different isoforms, but the few data available on this subject point to such a possibility. Different isoforms can show significant differences in their affinity for calmodulin (45) or in the pattern of phosphorylation (46). It is possible that these isoforms might display a differential distribution within the cell, as it has been shown in hepatocytes (47).

In summary, the present study shows that the initiation of the agonist-evoked Ca^{2+} signal is associated with complex changes in the plasma membrane Ca^{2+} transport systems. The increase of $[Ca^{2+}]_i$ following the release of Ca^{2+} from the intracellular Ca^{2+} stores rapidly (within 1 s) activates the PM Ca^{2+} extrusion system. The reported differences in the sensitivity to the levels of $[Ca^{2+}]_i$ and the different relationships between $[Ca^{2+}]_i$ and the rate of extrusion at the two functional poles of the pancreatic acinar cells (lumenal and basal) indicate that the plasma membrane Ca^{2+}ATPase might play an important role in the polarization of the Ca^{2+} response. The maximal "effective" depletion of the intracellular Ca^{2+} pools does not trigger immediately the activation of the Ca^{2+} entry pathway, suggesting the existence of a metabolic step interposed between these two processes.

Acknowledgments—E. C. T. thanks Prof. O. H. Petersen for his continuous support and interest during the stay in Liverpool and V. J. T. for showing and discussing new perspectives.

REFERENCES

1. Berridge, M. J. (1993) *Nature* **361,** 315–325
2. Kasai, H., and Augustine, G. J. (1990) *Nature* **348,** 735–738
3. Rooney, T. A., Sass, E., and Thomas, A. P. (1990) *J. Biol. Chem.* **265,** 10792–10796
4. Toescu, E. C., Lawrie, A. M., Petersen, O. H., and Gallacher, D. V. (1992) *EMBO J.* **11,** 1623–1629
5. Theler, J. M., Mollard, P., Guerineau, N., Vacher, P., Pralong, W. F., Schlegel, W., and Wolheim, C. B. (1992) *J. Biol. Chem.* **267,** 18110–18117
6. Thorn, P., Lawrie, A. M., Smith, P. M., Gallacher, D. V., and Petersen, O. H. (1993) *Cell* **74,** 661–668
7. Toescu, E. C., Gallacher, D. V., and Petersen, O. H. (1994) *Biochem. J.* **304,** 313–316
8. Kasai, H., Li, Y. X., and Miyashita, Y. (1993) *Cell* **74,** 669–677
9. Lawrie, A. M., Toescu, E. C., and Gallacher, D. V. (1993) *Cell Calcium* **14,** 698–710
10. van de Putt, F. H. M. M., De Pont, J. J. H. H. M., and Willems, P. H. G. M. (1994) *J. Biol. Chem.* **269,** 12438–12443
11. Petersen, C. C. H., Toescu, E. C., and Petersen, O. H. (1991) *EMBO J.* **10,** 527–533
12. Toescu, E. C., Lawrie, A. M., Gallacher, D. V., and Petersen, O. H. (1993) *J. Biol. Chem.* **268,** 18654–18658
13. Kasai, H. (1993) *Neurosci. Res.* **16,** 1–7
14. Tepikin, A. V., Voronina, S. G., Gallacher, D. V., and Petersen, O. H. (1992) *J. Biol. Chem.* **267,** 3569–3572
15. Muallem, S. (1989) *Annu. Rev. Physiol.* **51,** 83–105
16. Putney, J. W., Jr. (1990) *Cell Calcium* **11,** 611–624
17. Putney, J. W., Jr., and Bird, G. S. J. (1993) *Endocr. Rev.* **14,** 610–631
18. Hoth, M., and Penner, R. (1992) *Nature* **355,** 353–356
19. Fasolato, C., Hoth, M., and Penner, R. (1993) *J. Biol. Chem.* **268,** 20737–20740
20. Irvine, R. F. (1992) *FASEB J.* **6,** 3085–3091
21. Alvarez, J., Montero, M., and Garcia-Sancho, J. (1992) *FASEB J.* **6,** 786–792
22. Xu, X., Star, R. A., Tortorici, G., and Muallem, S. (1994) *J. Biol. Chem.* **269,** 12645–12653
23. Randriamampita, C., and Tsien, R. Y. (1993) *Nature* **364,** 809–814
24. Bird, G. S., and Putney, J. W. J. (1992) *J. Biol. Chem.* **268,** 21486–21488
25. Lee, K.-M., Toscas, K., and Villereal, M. L. (1993) *J. Biol. Chem.* **268,** 9945–9948
26. Llopis, J., Kass, G. E. N., Gahm, A., and Orrenius, S. (1992) *Biochem. J.* **284,** 243–247
27. Kass, G. E. N., Webb, D.-L., Chow, S. C., Llopis, J., and Berggren, P.-O. (1994) *Biochem. J.* **302,** 5–9
28. Toescu, E. C., and Petersen, O. H. (1994) *Pfluegers Arch.* **444,** 325–331
29. Elliot, A. C., Cairns, S. P., and Allen, D. G. (1992) *Pfluegers Arch.* **422,** 245–252
30. Tsien, R. W., and Tsien, R. Y. (1990) *Annu. Rev. Cell Biol.* **6,** 715–716
31. Iino, M., Yamazawa, T., Miyashita, Y., Endo, M., and Kasai, H. (1993) *EMBO J.* **12,** 5287–5291
32. Friel, D. D., and Tsien, R. W. (1992) *Neuron* **8,** 1109–1125
33. Miyazaki, S., Yuzaki, M., Nakada, K., Shirakawa, H., Nakanishi, S., Nakade, S., and Mikoshiba, K. (1992) *Science* **257,** 251–255
34. Berridge, M. J. (1994) *Biochem. J.* **302,** 545–550
35. Goldbetter, A., Dupont, G., and Berridge, M. J. (1990) *Proc. Natl. Acad. Sci. U. S. A.* **87,** 1461–1465
36. Kwan, C.-Y., Takemura, H., Obie, J. F., Thastrup, O., and Putney, J. W. J. (1990) *Am. J. Physiol.* **258,** C1006–C1015
37. Felder, C., Poulter, M. O., and Wess, J. (1992) *Proc. Natl. Acad. Sci. U. S. A.* **89,** 509–513

38. Kuno, M., and Gardner, P. (1987) *Nature* **326,** 301–304
39. Khan, A. A., Steiner, J. P., Kelin, M. G., Schneider, M. F., and Snyder, S. H. (1992) *Science* **249,** 1166–1168
40. Fadool, D. A., and Ache, B. W. (1992) *Neuron* **9,** 907–918
41. Koch, B. D., Faurot, G. F., Kopanitsa, M. V., and Swinney, D. C. (1994) *Biochem. J.* **302,** 187–190
42. Nathanson, M. H., Fallon, M. B., Padfield, P. J., and Maranto, A. R. (1994) *J. Biol. Chem.* **269,** 4693–4696
43. Petersen, C. C. H., Petersen, O. H., and Berridge, M. J. (1993) *J. Biol. Chem.* **268,** 22262–22264
44. Carafoli, E., and Stauffer, T. (1994) *J. Neurobiol.* **25,** 312–324
45. Enyedi, A., Filoteo, A. G., Gardos, G., and Penniston, J. T. (1991) *J. Biol. Chem.* **266,** 8952–8956
46. Strehler, E. E., Strehler-Page, M.-A., Vogel, G., and Carafoli, E. (1989) *Proc. Natl. Acad. Sci. U. S. A.* **86,** 6908–6912
47. Kessler, F., Bennardini, F., Bachs, O., Serratosa, J., James, P., Caride, A. J., Gazzotti, P., Penniston, J. T., and Carafoli, E. (1990) *J. Biol. Chem.* **265,** 16012–16019